Bull. Mater. Sci., Vol. 39, No. 7, December 2016, pp. 1691–1699. © Indian Academy of Sciences.
DOI 10.1007/s12034-016-1307-7

Corrosion and wear behaviour of multilayer pulse electrodeposited Ni–Al_2O_3 nanocomposite coatings assisted with ultrasound

H MAJIDI, M ALIOFKHAZRAEI*, A KARIMZADEH and A SABOUR ROUHAGHDAM
Department of Materials Science, Faculty of Engineering, Tarbiat Modares University, Tehran 1411713116, Iran

MS received 19 January 2016; accepted 15 April 2016

Abstract. **In this study, the Ni–Al_2O_3 nanocomposite multilayer coatings with six consecutive layers were electrodeposited on the mild steel by pulse electrodeposition with ultrasound agitation from nickel Watts-type bath. The structure and morphology of the etched coatings cross-section were characterized by scanning electron microscopy (SEM). The corrosion behaviour of these coatings was investigated in 1 M H_2SO_4 solution. All of the coatings showed the active–passive transition and the distinct difference in structure had negative influence on their corrosion resistance. Moreover, the tribological behaviour of these coatings was evaluated by pin-on-disc type. The results showed that wear resistance increased with increase in duty cycle and frequency.**

Keywords. **Pulse electrodeposition; Ni–Al_2O_3 nanocomposite coating; multilayer coatings; ultrasonic agitation.**

1. Introduction

Modern coating industry demands that the coatings for high mechanical and electrochemical properties be compared with conventional coatings. The multilayer coatings offer advantages to design the new coatings for improving performance. The multilayer composite coatings consist of two or more alternative layers with different compositions or structures that exhibit better enhanced oxidation resistance [1] as well as mechanical [2], electrochemical [3] and optical [4] properties compared to a single-layer coating. In addition, the multilayer coatings with lot of interfaces with the substrate, which can act as the barriers of dislocation motion, lead to increased mechanical properties. The multilayer coatings include ceramic/metal multilayer, such as Ti/TiN [5], W/WN [6], Al/AlN [7]; ceramic/ceramic multilayer, such as CrN/TiN [8], TiN/VN, TiN/NbN [9]; alloy multilayer, such as Cu–Ni [10], Ni–Cr [11], Cu/Cu-Co [12]; and composite multilayer, such as Ni–Al_2O_3 [13], produced by various methods such as chemical vapour deposition, physical vapour deposition, thermal plasma spray and electrodeposition. Owing to the relatively low deposition temperature, the low cost and ability to control the thickness of coatings, the electrodeposition method was widely used to electrodeposit nanocomposite coating for decades [14]. With the advances in electronics and microprocessor, the amount and form of the electrodeposition current applied can be controlled [15]. The pulse electrodeposition has interesting advantages, such as higher current density application, higher efficiency and more variable parameters, compared to the direct current density. Moreover, the composition [16] and microstructure [17] of composite coating can be controlled by the setting of pulse parameters, such as duty cycle, frequency and current density. Landolt and Marlot [18] showed that molybdenum content in Ni–Mo alloy was increased by increasing the pulse frequency at different duty cycles. In addition, the microstructures of the metal matrix such as texture, grain size and orientation was changed by changing pulse parameters [19,20]. However, in the industrial units the cost of pulse equipment is more expensive than DC units, due to its complicated and sophisticated design. In addition, many aspects of pulse electrodeposition have not been well-known [21]. The main challenge to the production of nanocomposite coatings is the agglomeration of the nanoparticles in solution bath and coating due to their high free energy surface. The various chemical and mechanical methods such as magnetic stirring use additives, while the application of pulse electrodeposition and ultrasound agitation, etc. are used to solve this problem. The additives such as saccharin and sodium dodecyl sulphate in the electrolyte were found to change microstructure, surface roughness, brightness and particles content in the nanocomposite coatings. The ultrasound agitation was significantly attended to disperse nanoparticles in solution bath. In addition, ultrasound generates the acoustic cavitation in liquid media that enhances the incorporation and dispersion of nanoparticles in the metal matrix and affected coating microstructure and surface morphology [22]. The Ni–Al_2O_3 nanocomposite coatings were widely studied due to their hardness and wear and corrosion resistance compared to electrodeposited pure nickel coatings [23]. The researchers have focused on the effect of pulse parameters on the increase and dispersion of the alumina nanoparticles in the nickel matrix. The functionally graded Ni–Al_2O_3 nanocomposite coatings and the structures and the amount of the alumina nanoparticles that gradually change in the cross-section of

*Author for correspondence (khazraei@modares.ac.ir, maliofkh@gmail.com)

the coatings were synthesized and studied, but the multilayer Ni–Al_2O_3 nanocomposite coatings with two or more layers that alternatively change in the cross-section of the coating are novel [13].

In this study, we electrodeposited Ni–Al_2O_3 nanocomposite multilayer coatings that consisted of two alternative layers in different duty cycles at step-like frequency 100–1000 Hz and in different frequency with step-like duty cycle 20–80% conditions from Watts bath in the presence of ultrasound. In addition, a comparative study of the effects of the frequency and duty cycle on the morphology, electrochemical and tribological behaviours of the Ni–Al_2O_3 nanocomposite multilayer coatings were investigated.

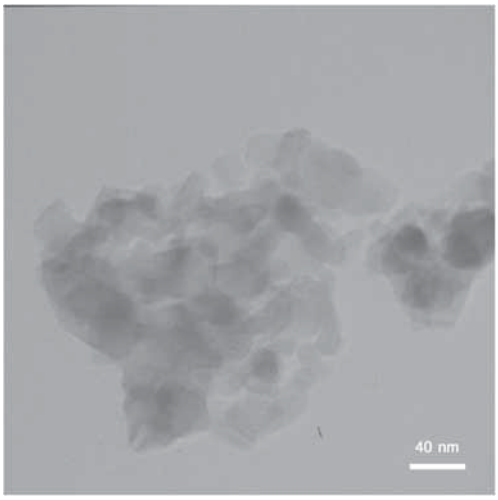

Figure 1. TEM image of Al_2O_3 nanoparticles.

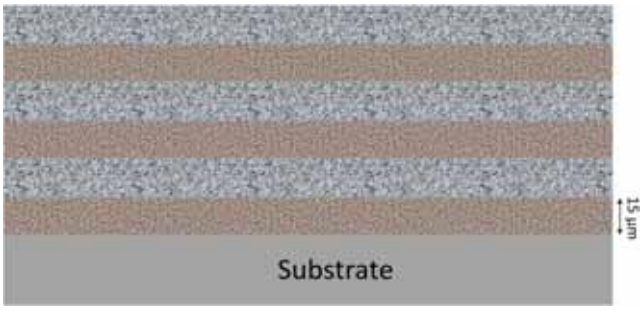

Figure 2. The schematic representation of alternative layers in cross-section of the coatings.

2. Experimental

Nickel–alumina multilayer nanocomposite coatings were electrodeposited from acidic nickel sulphate bath (250 g l^{-1} $NiSO_4{\cdot}6H_2O$, 40 g l^{-1} $NiCl_2{\cdot}6H_2O$ and 35 g l^{-1} H_3BO_3), to which 50 g l^{-1} alumina nanopowder was added. Figure 1 shows the transmission electron microscopy image of Al_2O_3 nanoparticles. The homogeneous suspension of alumina in Watts bath was maintained by using magnetic stirring at the speed of 300 rpm for at least 24 h before deposition and then the solution was agitated by ultrasound homogenizer (TOPSONIC 400 W, 20 kHz). The frequency and power of ultrasound homogenizer were 20 kHz and 150 W (25% max. power), respectively, for 200 cc of the bath solution for 30 min. Mild steel plate with an area of 20 cm^2 was used as the cathode. A high purity (99.75%) nickel plate was used as the anode. Before electroplating, cathodes were polished by fine emerge paper up to 1200 grades and then were washed in distilled water, activated in HCl (15%) for 60 s, washed in distilled water again and then immediately immersed in plating bath to deposit nanocomposite coating. Moreover, suspension solution was subjected to mechanical agitation either by magnetic stirrer (150 rpm) or an ultrasound homogenizer (90 W).

Each of the multilayer coatings used in this study was produced at an average current density of 5 A dm^{-2} and at alternative different pulse conditions. To study the role of frequency in the production of multilayer coatings, a set of samples was prepared with step-like duty cycle of 20–80% and fixed frequency of 100, 550 and 1000 Hz. Also to study the effect of duty cycle in multilayer coatings a set of samples was prepared with step-like frequency of 100–1000 Hz at fixed duty cycle of 20, 50 and 80%. The schematic representation of multilayer composite coating has been presented in figure 2. Details of pulse parameters for these samples are presented in table 1.

The cross-section of the coatings was etched by the solution composed of 50 ml nitric acid and 50 ml acetic acid. The etched cross-section, the surface morphology and the nanoparticle content of multilayer nanocomposite coatings were investigated by a field emission scanning electron microscopy (FE-SEM, TESCAN MIRR3 LMU). The tribological properties of the multilayer composite coatings were carried out by using a pin-on-disc type wear tester according to ASTM G 99. Alumina ball was used for the pin material (counterpart material: 7 mm). Wear test specimen size was

Table 1. Sample deposition conditions used to study the fabrication of multilayer composite coating.

Sample	f (Hz)	θ (%)	T_{off} (ms)	T_{on} (ms)	i_p (A dm^{-2})
f_{100}	100	20–80–20–80–20–80	8–2	2–8	25–6.25
f_{550}	550	20–80–20–80–20–80	1.4–0.36	0.36–1.4	25–6.25
f_{1000}	1000	20–80–20–80–20–80	0.8–0.2	0.2–0.8	25–6.25
D_{20}	100–1000–100–1000–100–1000	20	8–0.8	2–0.2	25
D_{50}	100–1000–100–1000–100–1000	50	5–0.5	5–0.5	10
D_{80}	100–1000–100–1000–100–1000	80	2–0.2	8–0.8	6.25

$2.5 \times 2.5 \times 1$ mm^3. Before wear testing, the coatings were polished with emerge paper 2000#, degreased, washed with distilled water and then dried. The tribology study was performed under a 40-kgf load at room temperature in the air with the sliding speed of 90 rpm. The wear track radiuses were 1.1 and 1.7 cm for evaluating their wear rate and coefficient of friction, respectively. The weight loss of specimen was weighed before and after the test.

The potentiodynamic measurements of the multilayer Ni–Al_2O_3 composite coatings were performed in a 1 M solution of H_2SO_4 at room temperature (25 ± 2°C). Before the electrochemical investigations, the surface of the Ni–Al_2O_3 composite coatings was polished with emerge paper 2000#, washed with distilled water, degreased with methanol and then washed in distilled water again. The surface area of the working electrode was 0.785 cm^2. A saturated calomel electrode KCl was used as the reference electrode and a platinum gauze was used as counter electrode. The polarization potentiodynamic curves were recorded after 30 m of immersion. The rate of potential changes was set at 0.5 mV s^{-1}.

3. Results

3.1 *SEM examinations*

Figure 3 shows the SEM backscatter electron images of etched cross-section of the samples produced under the step-like duty cycle of 20–80% (layer I at duty cycle of 20% and layer II at duty cycle of 80%) at the different frequencies of 100, 550 and 1000 Hz and the step-like frequency 100–1000 Hz (layer I at frequency of 100 Hz and layer II at frequency of 1000 Hz) at different duty cycles of 20, 50 and 80%. As indicated in figure 3, the cross-section of coatings includes six consecutive layers, and the multilayer composite coating produced under the step-like changing of duty cycle of 20–80% at the low frequency of 100 Hz revealed further structural differences between the layers than those at the high frequency of 1000 Hz. Further, the coating produced under the step-like changing of the frequency of 100–1000 Hz at the low duty cycle of 20% indicated further structural differences between the layers than those at the high duty cycle of 80%. In addition, the interface between the layers was faded by the increase in either duty cycle or frequency. This result may be related to the change in the orientation and grain size of nickel matrix. This is in good agreement with other researches [13,19]. Chen *et al* [19] have reported that increase in frequency from 10 to 1000 Hz at duty cycle of 50% resulted in a change in the strong (111) preferred orientation compared to the (200) random orientation. Hence, the surface energy of (200) plane is higher than that of the (111) plane due to its low planar density. Lajevardi *et al* [13] also showed that continuous decrease in duty cycle resulting from 90 to 10% at different frequencies changed the microstructure of the composite coating to small randomly oriented grains. The structural difference between the layers can also be attributed to the fact that the nucleation and growth of matrix grain are affected by peak current density. At the constant average current density, decrease in duty cycle increases peak current density that leads to increased nucleation rate resulting in finer grain size. In other words, the layers with low duty cycles are inclined to further etching than the

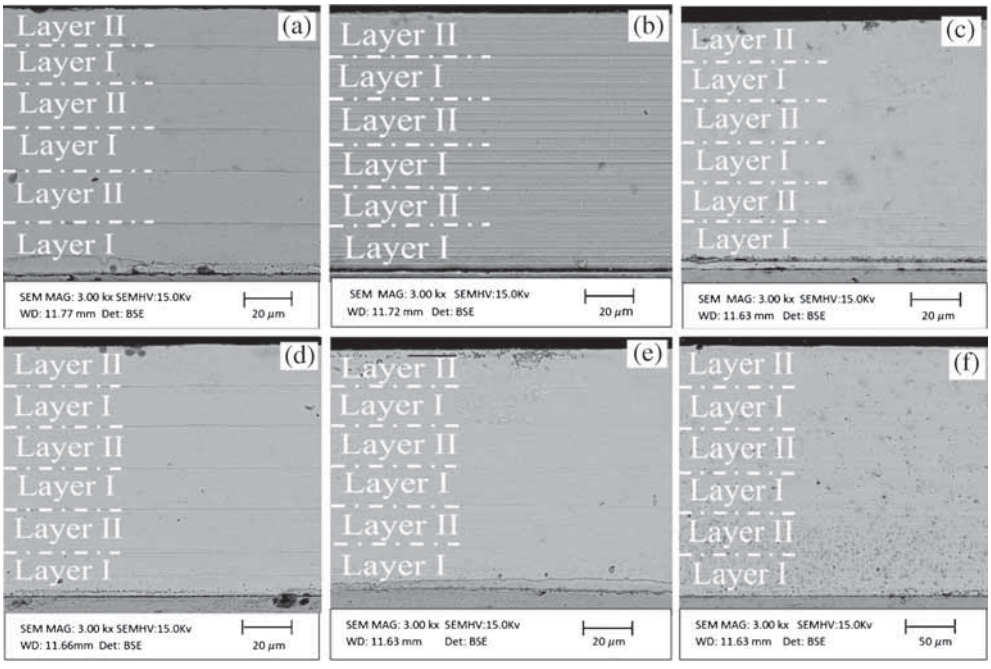

Figure 3. SEM (backscattered electron) images of etched cross-section for samples produced under the alternative step-like duty cycle 20–80% at (**a**) $f = 100$, (**b**) 550 and (**c**) 1000 Hz and for samples of the alternative step-like frequency 100–1000 Hz at (**e**) DC = 20, (**f**) 50 and (**g**) 80%.

layers with high duty cycles. However, this structural difference between the layers produced under the step-like frequency of 100–1000 Hz at high duty cycles decreased. By increasing frequency, the coatings tend to be further etched due to high ratio of the preferred orientation to the random orientation at high frequencies. In addition, the increase in frequency fades the structural difference between the layers so that the layers of coating are uniformly etched. Bahrololoom and Sani [24] reported that the properties of nickel–alumina composite coatings are more affected by the duty cycle rather than frequency.

The square pulse current as a function of time is shown in figure 4. By using Fourier series, it is possible to write the electrodeposition pulse parameters in an equation. The Fourier series for square-wave pulse electrodeposition is given by

$$i(t) = i_a + \frac{i_a}{\pi\theta}\sum_{m=1}^{\infty}\left[\left(\frac{(1-\cos(2m\theta\pi))}{m}\right)\sin(2m\pi ft) + \left(\frac{\sin(2m\theta\pi)}{m}\right)\cos(2m\pi ft)\right], \quad (1)$$

where i, i_a, θ, f and t are current density, average current density, duty cycle, pulse frequency and time, respectively. At the constant average current density, Equation 1 shows that the duty cycle and frequency changed the current amplitude and period of applied current density, respectively. The peak current density is an important parameter in the charging and discharging of the electrical double layer, in which the charging and discharging time is decreased by increasing peak current density [25]. In other words, the increase in peak current density due to decreased duty cycle can support the high frequencies.

Table 2 shows the percentage volume of the co-deposited alumina particles in the alternative layers of composite coatings as a function of the duty cycle and frequency. It is obvious that the alumina content in layers is increased by increasing frequency and decreasing duty cycle. By increasing frequency the off-time pulse becomes shorter, then more alumina particles can most probably absorb the cathode surface under ultrasonic agitation. Bahrololoom *et al* [24] reported that increasing the frequency leads to slight decrease in alumina particles in the coatings. While Chen *et al* [19] showed that the amount of the alumina particles was increased by increasing frequency, it can be related to the difference in the electro co-depositing mechanism of inert particles in the coatings.

The Celis's model [26] for the co-deposition mechanism of inert particles in the metal matrix is based on the formation of the ions layer surrounding the particles, transfer of the particles to cathode surface by hydrodynamic forces and diffusion and trap in the reduction layer on the cathode surface. In fact,

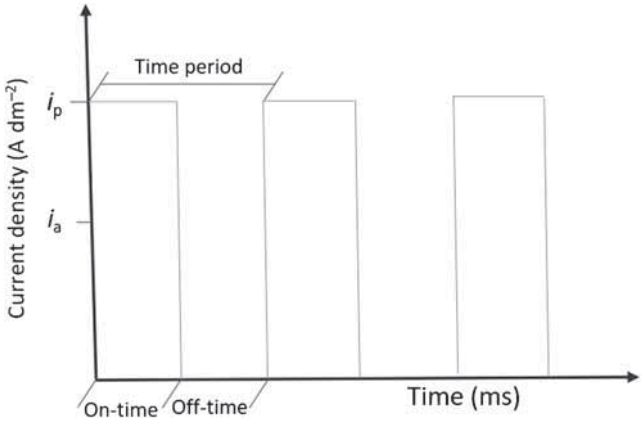

Figure 4. Square pulse-current waveform.

Table 2. Volume percentage of co-deposited alumina particles in the layers of different samples.

Sample	Co-deposited Al_2O_3 of layer (vol%)	
	Layer I	Layer II
f_{100}	4.4	2.4
f_{550}	5.6	2.8
f_{1000}	5.9	3.7
D_{20}	4.5	6.4
D_{50}	4.1	5.2
D_{80}	3.2	3.5

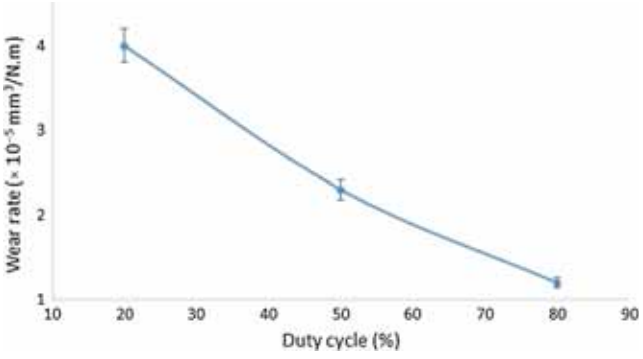

Figure 5. Effect of frequency on the wear rate of Ni–Al_2O_3 multilayer nanocomposite coatings prepared under step-like duty cycle of 20–80%.

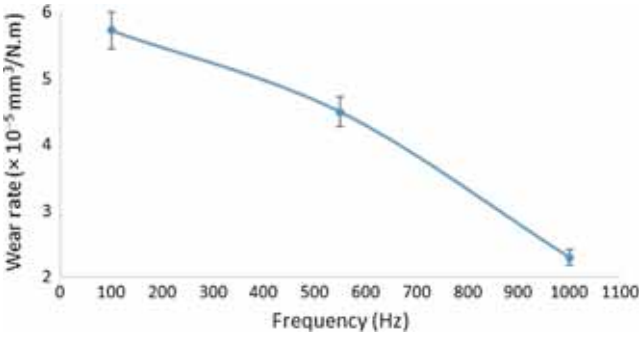

Figure 6. Effect of duty cycle on the wear rate of Ni–Al_2O_3 multilayer nanocomposite coatings prepared under step-like frequency of 100–1000 Hz.

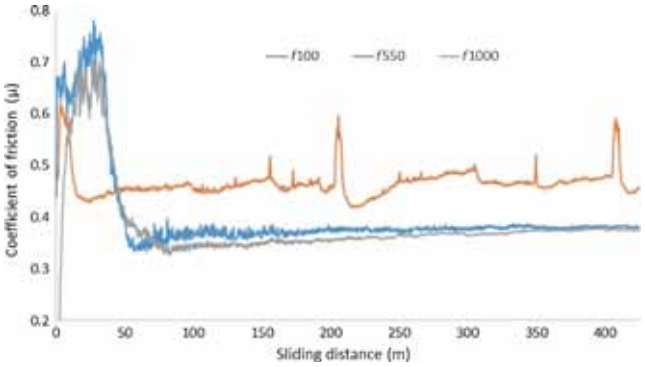

Figure 7. The coefficient of friction *vs.* sliding distance for the composite coatings prepared under step-like duty cycle of 20–80% at different frequencies of 100, 550 and 1000 Hz.

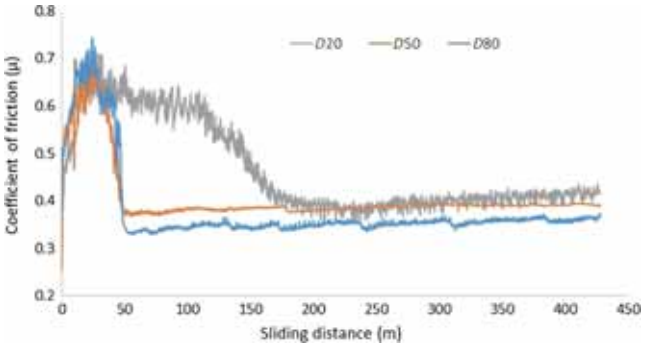

Figure 8. The coefficient of friction *vs.* sliding distance for the composite coatings prepared under step-like frequency of 100–1000 Hz at different duty cycles of 20, 50 and 80%.

according to the Celis's model, the amount of particles in the coatings depends on the electrodeposition hydrodynamic and diffusion conditions. In this study, the hydrodynamic and diffusion conditions were neglected by using high power ultrasound and magnetic agitation during electrodeposition and high particle concentration. Therefore, increasing the peak current (i.e., decreasing duty cycle) leads to high driving force for trapping the alumina particles in nickel matrix, as shown in table 2. At a fixed frequency, the longer T_{off} at a low duty cycle provides more possibility for Al_2O_3 nanoparticles to reach the cathode surface, increasing the amount of adsorbed alumina particles to deposit in the coating.

This study also shows that the amount of the deposited Al_2O_3 particles increases with the pulse frequency (table 2). During pulse electrodeposition, the higher frequency could generate more overpotential, providing more energy for the absorption of inert particles such as alumina.

3.2 *Tribological behaviour*

The relationships between wear rate and frequency and duty cycle in pulse electroplated Ni–Al_2O_3 multilayer nanocomposite are illustrated in figures 5 and 6. In general, the wear rate of the nanocomposite coating with inert particles depends on applied load [27]; pin characteristics, such as hardness and radius, sliding speed and distance; sliding types, such as dry and lubricated [28]; structure and hardness of coating matrix; particle content and its distribution [29]. The structure and hardness of coating matrix, content and the distribution of particles affect the wear mechanism.

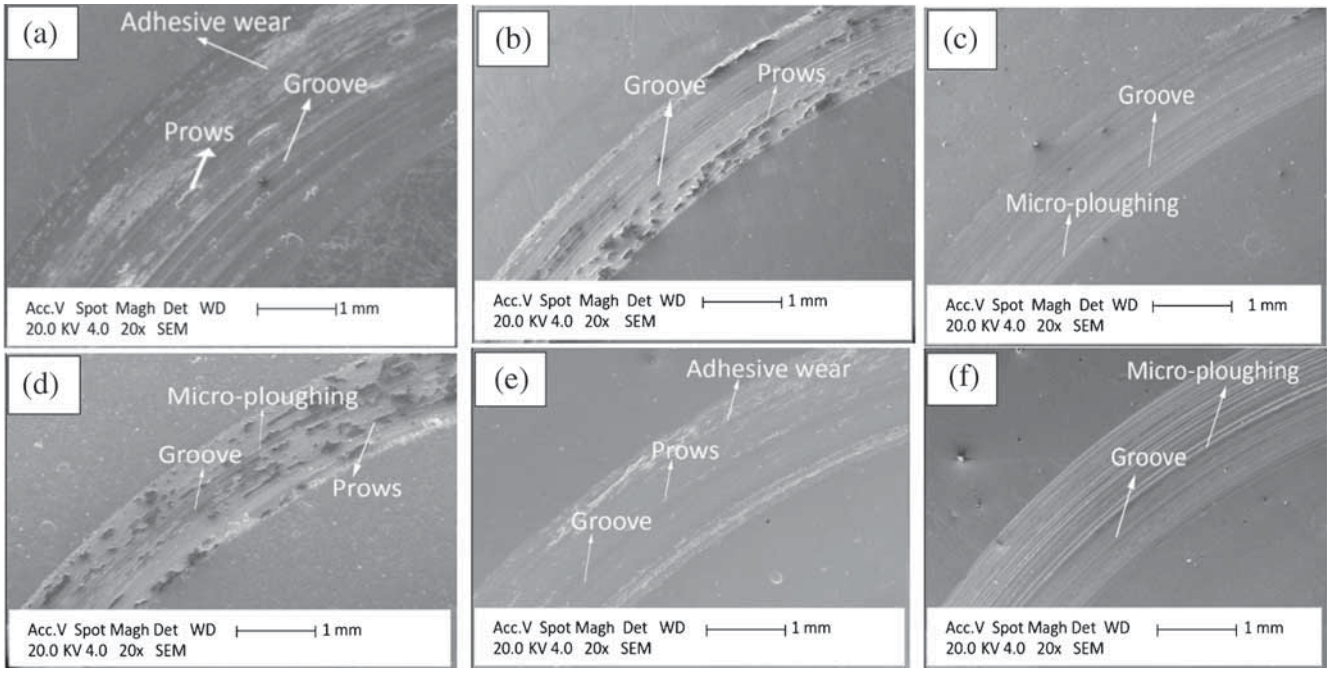

Figure 9. The backscatter electron image of the worn surface under dry sliding of the multilayer composite coatings produced under step-like duty cycle of 20–80% at frequencies of (**a**) 100, (**b**) 550 and (**c**) 1000 Hz, and under step-like frequency of 100 and 1000 Hz at duty cycles of (**d**) 20, (**e**) 50 and (**f**) 80%.

Figure 5 shows that the wear rate of the coatings were decreased by increasing duty cycle. Also, as seen in figure 6, increasing frequency resulted in a decline in the wear rate. It can be related to the fact that the distinct difference in the structures of the layer has negative effect on wear resistance. This distinct difference in the structure of the layers may reduce the shear strength in the interfaces of the layers and split the layers [30].

Figures 7 and 8 show the friction coefficient of multilayer Ni–Al_2O_3 nanocomposite coatings under different pulse electrodeposition conditions and dry condition at 40 N force and room temperature. The worn coating surfaces were examined to study the wear mechanism. Figure 9 shows the surface morphology of the coating after wear test. As shown in figure 9, the fracture surface of the worn surface, large groove and prows in the worn surface of the coating were produced under frequency of 100 Hz at step-like duty cycle 20–80%. As seen in figure 9, the worn surface at the frequency of 100 Hz clearly indicates the combination of severe adhesive and abrasive wear. It corresponds to the higher coefficient of friction shown in figure 7. By increasing the frequency to 550 Hz, the wear mechanism indicates the combination of adhesive and abrasive wear with small grooves so that its coefficient of friction slowly reaches the steady region (figure 7). By increasing the frequency to 1000 Hz, small grooves and ploughings of its worn surface were formed, indicating abrasive as the prominent wear mechanism and obviously showing that the coating matrix can be capable of supporting the loading force of 40 N in speed sliding of 5.8 m s^{-1}. Furthermore, its friction coefficient quickly reached the steady region that may be related to its high plastic deformation capacity (figure 7).

Figure 9 shows the worn surfaces of the multilayer composite coatings prepared under the step-like frequency of 100–1000 Hz at different duty cycles of 20, 50 and 80%. By increasing duty cycle, the wear rate decreased in an approximately linear manner. It can also be related to decrease in structural difference of the layers and may be related to increase in the nanoparticle content in layers. By comparing figures 7 and 8 with figure 9, it shows that the friction coefficient of these coatings is increased by increase in the real contact area between alumina ball and coatings during dry sliding. As shown in figure 9, increase in the duty cycle changed the wear mechanism from combination of sever abrasive and adhesive wear to soft abrasive wear at the duty cycle of 80%. The high friction coefficient of samples f_{100} and D_{20} may be related to the increased contact area between alumina ball and coating surface during dry sliding wear. It can be the case that their grooves are widely compared to other samples.

The present paradox in the tribological results reported by other researchers [31] may be attributed to the fact that the wear and the coefficient of friction are not characterization of materials but depend on tribo-system conditions. In addition, it can be attributed to the complex hydrodynamic electroplating conditions such as particle concentration, stirrer and ultrasonic agitation, difference in applied pulse parameters and the design of coatings such as thickness, the agglomeration of particles and the structure of the layers.

3.3 *Corrosion resistance*

The polarization curves for the multilayer Ni–Al_2O_3 nanocomposite coatings immersed in a 1 M solution of H_2SO_4 are shown in figures 10 and 11. The corrosion potentials (E_{corr}), corrosion current densities (i_{corr}), the anodic and the cathodic tafel slopes (B_a and B_c) extracted from the slope of the curves are shown in table 3. The polarization resistance (R_p) was measured from the Stern-Geary equation, as follows:

$$R_p^{-1} = 2.303 i_{corr}\left(\frac{1}{B_a} + \frac{1}{B_c}\right), \quad (2)$$

R_p shows the polarization resistance of the metal to uniform corrosion in a homogenous environment.

All multilayer Ni–Al_2O_3 nanocomposite coatings exhibited active–passive-transpassive behaviour. As shown in figures 10 and 11, the initial thin passive films were in extensively unsteady state in the critical passive current density

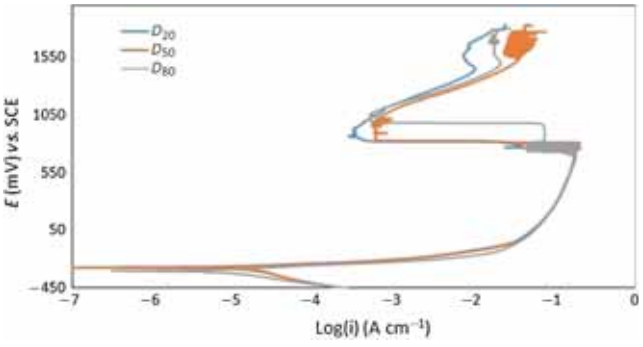

Figure 10. Potentiodynamic polarization curves of multilayer Ni–Al_2O_3 nanocomposite with alternative step-like frequncy of 100–1000 Hz at different duty cycles of 20, 50 and 80% in 1 M H_2SO_4 at scan rate of 0.5 m V^{-1}.

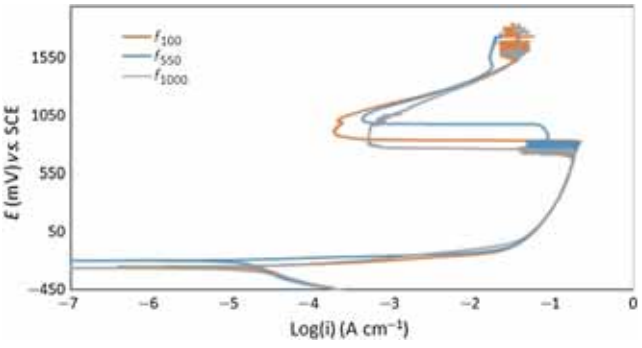

Figure 11. Potentiodynamic polarization curves of multilayer Ni–Al_2O_3 nanocomposite with alternative step-like duty cycle of 20–80% at different frequncies of 100, 500 and 1000 Hz in 1 M H_2SO_4 at scan rate of 0.5 m V^{-1}.

that can be related to the defective nature of passive film on nickel [32,33]. Figure 12 illustrates the SEM images of the corroded surface of composite coatings in 1 M H_2SO_4 solution. Many corrosion pits appear on the composite surfaces. The high number of defects in the passive film lead to low passive range. Hence nickel cations easily move through the passive films and lead to break and remove passive films. The coatings had approximately the same critical passive current density. As seen in table 3, the polarization resistance of multilayer nanocomposite coatings was increased by increasing the duty cycle and frequency.

In general, the present distinct layers in the composite coatings have more negative effects on their corrosion resistance due to the formation of defects such as dislocation in the interface of the layers, which act as the chemical heterogeneities in the corrosion processes [33]. The inert particles in composite coatings have two opposite effects on the composite corrosion resistance: the positive effect is that the co-deposited inert particles in the metal matrix lead to decreased grain size and pit corrosion [34] and the negative effect is that the presence of the inert particles in the coating generates dislocation and defects in metal matrix, which act as preferred places for corrosion process [35]. By increasing frequency, the polarization resistance of the coatings was increased. It may correspond to the fact that increase in the frequency increased nanoparticles and decreased the distinct difference in the structure of layers. The nanoparticles act as a corrosion barrier due to their inert electrochemical properties [34]. It can be concluded that the distinct structures in the layers had more significant influence on the electrochemical behaviour of the multilayer Al_2O_3–Ni nanocomposite coatings than the amount of the alumina nanoparticles in their layers. The alumina nanoparticles embedded in nickel grain borders and in the grain can accelerate the passive processes [36].

Table 3. Polarization resistance of Al_2O_3–Ni multilayer composite coatings evaluated from polarization potentiodynamic curves obtained in solution of 1 M H_2SO_4.

Sample	E_{corr} (mV)	i_{corr} (μA cm^{-2})	B_a (mV dec)	B_c (mV dec)	R_p (Ω cm^2)
f_{100}	−252	20	29	223	557
f_{550}	−198	10	23	219	904
f_{1000}	−262	16	45	173	970
D_{20}	−270	16	41	190	915
D_{50}	−275	13	35	158	957
D_{80}	−302	6	39	97	2013

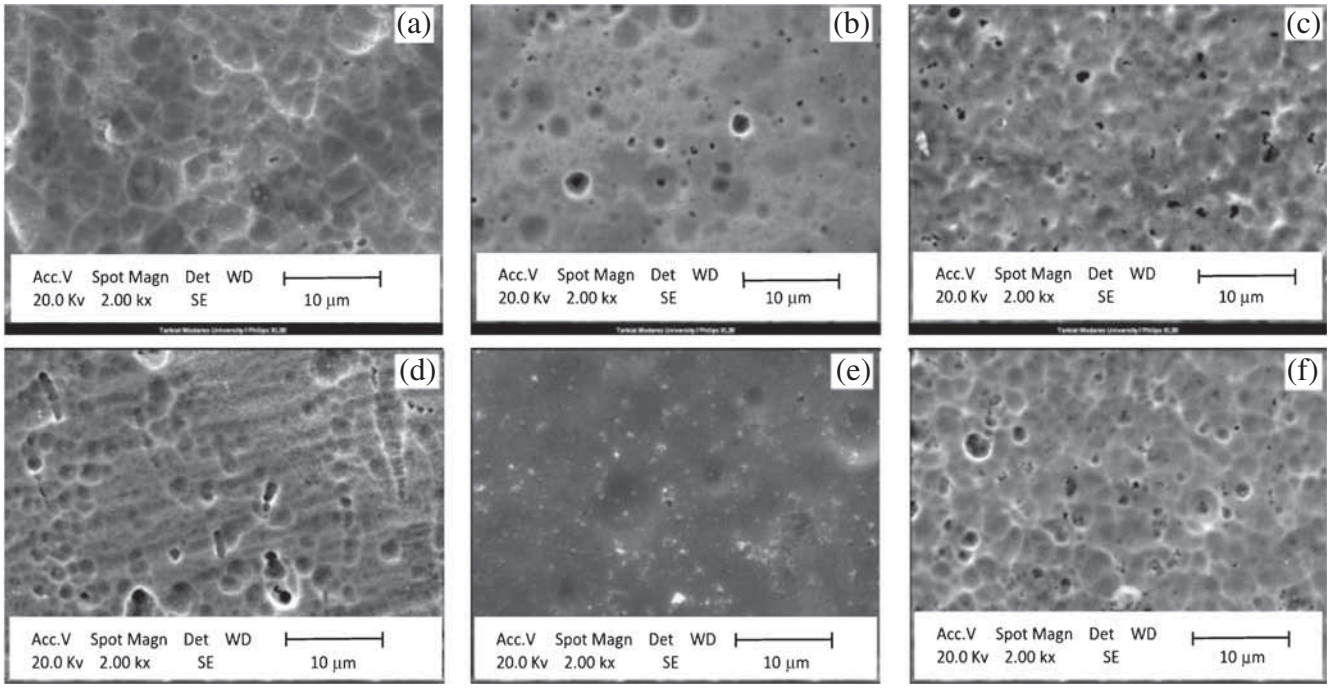

Figure 12. SEM (secondary electron) images of corroded surface for composite coatings after potentiodynamic measurements in 1 M solution of H_2SO_4 at room temperature (25 ± 2°C).

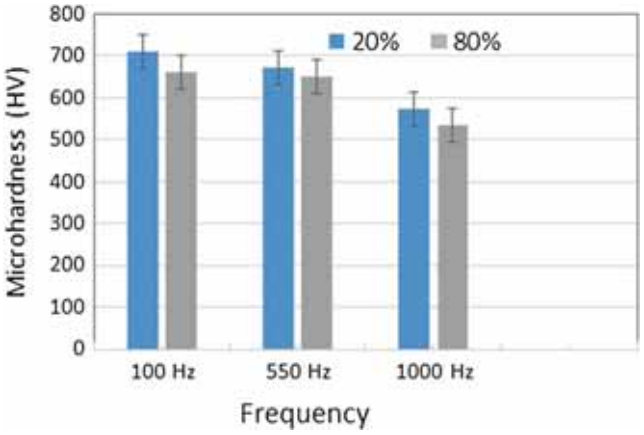

Figure 13. The effect of pulse frequency and duty cycle on the microhardness of the composite coating layers.

3.4 *Microhardness*

Figure 13 shows the microhardness of the nanocomposite coating layers. The microhardness of the coating layers was decreased with increase in the duty cycle. The same results have been reported by other researchers [13,24]. It can be related to this fact that the decrease in duty cycle at constant frequency increases T_{off}. Therefore, it is possible that nanoparticle exposure increases near the cathode surface. On the other hand, the microhardness of the composite coatings was decreased by increasing frequency. It can be related to the change preferred from crystal orientation to random crystal orientation [13,19]. The contradictory results were obtained by Bahrololoom *et al* [24] that they can be explained by alumina particles size and pulse frequency range. In general, the strengthening mechanism of the composite coatings can be described as follows [37,38]: (a) particle strengthening that is related to hard particle volume fraction above 20%; (b) dispersion strengthening that is associated with fine grain (<1 μm) volume fraction lower than 15%; (c) grain refinement strengthening described by Hall-Petch relationship; (d) crystal orientation that is related to change microhardness and plastic deformation in different crystal orientations. As said above, Bahrololoom *et al* [24] have used alumina particles with the average size of 5 μm, while other researchers have used alumina particle with submicron.

4. Conclusions

The Ni–Al_2O_3 multilayer composite coatings with six alternative layers were prepared by pulse electrodeposition. The coatings were electrodeposited on mild steel under the step-like duty cycle of 20–80% at different frequencies of 100, 550 and 1000 Hz, and also under the step-like frequency of 100–1000 Hz at different duty cycles of 20, 50 and 80%. SEM images showed that the etched cross-sections of the coatings had laminar and alternative structures. The incorporated alumina in the layers was increased by increasing frequency and decreasing duty cycle. The distinct structure of the layers was negative in the tribological and electrochemical behaviour of the coatings. The wear resistance of the coatings was increased by increasing the duty cycle and frequency. Duty cycle has more pronounced effect on the coating properties such as wear and corrosion resistance than frequency.

References

[1] Koller C, Hollerweger R, Rachbauer R, Polcik P, Paulitsch J and Mayrhofer P 2013 18th plansee seminar

[2] Riedl H, Koller C M, Limbeck A, Kalaš J, Polcik P and Mayrhofer P H 2015 *J. Vac. Sci. Technol.* **A33** 05E129

[3] Torabinejad V, Rouhaghdam A S, Aliofkhazraei M and Allahyarzadeh M 2016 *J. Alloys Compd.* **657** 526

[4] Raut H K, Ganesh V A, Nair A S and Ramakrishna S 2011 *Energy Environ. Sci.* **4** 3779

[5] Kot M, Major L, Rakowski W and Lackner J 2012 *J. Balk. Tribol. Assoc.* **18** 92

[6] Maillé L, Aubert P, Sant C and Garnier P 2004 *Surf. Coat. Technol.* **180** 483

[7] Zhang G, Wu Z, Wang M, Fan X, Wang J and Yan P 2007 *Appl. Surf. Sci.* **253** 8835

[8] Major L, Morgiel J, Lackner J, Szczerba M, Kot M and Major B 2008 *Adv. Eng. Mater.* **10** 617

[9] Kim S H, Baik Y J and Kwon D 2004 *Surf. Coat. Technol.* **187** 47

[10] Troyon M and Wang L 1996 *Appl. Surf. Sci.* **103** 517

[11] Etminanfar M and Sohi M H 2012 *Thin Solid Films* **520** 5322

[12] Kelly J, Bradley P and Landolt D 2000 *J. Electrochem. Soc.* **147** 2975

[13] Lajevardi S, Shahrabi T and Szpunar J 2013 *Appl. Surf. Sci.* **279** 180

[14] Thiemig D, Bund A and Talbot J B 2009 *Electrochim. Acta* **54** 2491

[15] Chandrasekar M and Pushpavanam M 2008 *Electrochim. Acta* **53** 3313

[16] Datta M and Landolt D 2000 *Electrochim. Acta* **45** 2535

[17] Cohen U, Koch F and Sard R 1983 *J. Electrochem. Soc.* **130** 1987

[18] Landolt D and Marlot A 2003 *Surf. Coat. Technol.* **169** 8

[19] Chen L, Wang L, Zeng Z and Xu T 2006 *Surf. Coat. Technol.* **201** 599

[20] Thiemig D, Lange R and Bund A 2007 *Electrochim. Acta* **52** 7362

[21] Chandrasekar M and Pushpavanam M 2008 *Electrochim. Acta* **53** 3313

[22] García-Lecina E, García-Urrutia I, Díez J, Morgiel J and Indyka P 2012 *Surf. Coat. Technol.* **206** 2998

[23] Szczygieł B and Kołodziej M 2005 *Electrochim. Acta* **50** 4188

[24] Bahrololoom M and Sani R 2005 *Surf. Coat. Technol.* **192** 154

[25] Puippe J-C and Leaman F 1986 *Theory and practice of pulse plating* (Orlando: Amer. Electroplaters Soc.)

[26] Celis J-P, Roos J and Buelens C 1987 *J. Electrochem. Soc.* **134** 1402

[27] Akinci A, Sen S and Sen U 2014 *Compos. Part B: Eng.* **56** 42
[28] Cai P, Wang T and Wang Q 2016 *Tribol. Trans.* **59** 28
[29] Al-Samarai R A, Haftirman K R A and Al-Douri Y 2012 *IJSR* **2** 1
[30] Holmberg K, Matthews A and Ronkainen H 1998 *Tribol. Int.* **31** 107
[31] Kato K 2000 *Wear* **241** 151
[32] Rofagha R, Splinter S, Erb U and McIntyre N 1994 *Nanostruct. Mater.* **4** 69
[33] Mishra R and Balasubramaniam R 2004 *Corrosion Sci.* **46** 3019
[34] Sajjadnejad M, Mozafari A, Omidvar H and Javanbakht M 2014 *Appl. Surf. Sci.* **300** 1
[35] Hovestad A and Janssen L 1995 *J. Appl. Electrochem.* **25** 519
[36] Shi L, Sun C, Gao P, Zhou F and Liu W 2006 *Appl. Surf. Sci.* **252** 3591
[37] Robin A and Fratari R 2007 *J. Appl. Electrochem.* **37** 805
[38] Aal A A 2008 *Mater. Sci. Eng. A Struct. Mater.* **474** 181